

The Electroweak Chiral Lagrangian and CP-Violating Effects in Technicolor Theories

Thomas Appelquist and Guo-Hong Wu
Department of Physics, Yale University, New Haven, CT 06520

June 28, 1994

Abstract

We estimate the CP-violating $WW\gamma$ and WWZ anomalous form factors, arising from CP-violating interactions in extended technicolor theories, and discuss their future experimental detectability. The electric dipole moment of the W boson is found to be as large as $\mathcal{O}(10^{-21})$ e cm. We connect the CP-odd $WW\gamma$ and WWZ couplings to the corresponding CP-violating electroweak chiral lagrangian operators. The electric dipole moments of the neutron and the electron in technicolor theories are estimated to be as large as $\mathcal{O}(10^{-26})$ e cm and $\mathcal{O}(10^{-29})$ e cm respectively. We also suggest the potential to observe large CP-violating technicolor effects in the decay $t \rightarrow b + W^+$.

1 Introduction

Recent work on extended technicolor (ETC) model building [1, 2] has demonstrated that technicolor (TC) theories could survive the challenges posed by precision electroweak measurements, the fermion mass spectrum, and limits on flavor-changing neutral currents and various rare decay modes. However, CP violation in technicolor theories remains a puzzling problem despite much study beginning more than ten years ago [3]. In this paper we reexamine this problem in a generic ETC model, with attention focused on the CP-odd $WW\gamma$ and WWZ anomalous interactions and their induced effects.

The electroweak symmetry breaking sector in technicolor theories can be

most conveniently parameterized below the breakdown scale of chiral perturbation theory Λ_χ by a gauged nonlinear chiral lagrangian [4, 5]. The scale Λ_χ is approximately given by [6],

$$\Lambda_\chi \simeq \frac{4\pi f}{\sqrt{N_f}}, \quad (1)$$

where $f = \frac{(\sqrt{2}G_F)^{-\frac{1}{2}}}{\sqrt{N_f/2}} \simeq \frac{250}{\sqrt{N_f/2}}$ GeV is the Goldstone boson decay constant, and where N_f is the number of technifermion flavors ($N_f/2$ is the number of technifermion weak doublets). Restricting attention to the minimal $SU(2)_L \times SU(2)_R$ chiral symmetry of the technifermions and imposing electroweak gauge invariance, thirteen CP-conserving and three CP-violating operators up to dimension-four¹ can be written down after using the classical equations of motion [4, 7]. The electroweak S , T and U parameters [8], and the CP-even and CP-odd $WW\gamma$ and WWZ couplings [9], can all be conveniently described by these operators of the electroweak chiral lagrangian [7].

When extended to a larger global symmetry (as in the one family TC model to be used in this paper), there will be pseudo-Goldstone-bosons (PGBs) appearing as effective degrees of freedom of the electroweak chiral lagrangian, and more operators can be written down beyond those for the minimal $SU(2)_L \times SU(2)_R$ chiral symmetry. These additional operators will not, however, generate any new interactions at tree level among the electroweak gauge bosons, beyond those already existing in the gauged $SU(2)_L \times SU(2)_R$ chiral lagrangian. In this paper, we will concentrate on the anomalous interactions among the electroweak gauge bosons. In particular, we will study the effects of CP-violating, ETC interactions on the triple-gauge-boson vertices (TGV's) measured below Λ_χ . As the strength

¹Dimension counting of the electroweak chiral lagrangian operators will be explained in section 2.

of the vertices involving PGBs is expected to be the same as those involving only electroweak gauge bosons, the contribution of the PGBs to the CP-odd TGVs will be suppressed by at least $\frac{\alpha}{\pi}$ (α is the fine structure constant) relative to the direct contribution from the CP-violating ETC interactions. We will therefore ignore the PGBs in this paper, and will restrict attention to the gauged $SU(2)_L \times SU(2)_R$ electroweak chiral lagrangian.

The size of the CP-violating dimension-four operators of the chiral lagrangian depends on the details of the high energy ETC sector, and simple dimensional estimates may not be trustworthy. Besides the suppression factor $\frac{\Lambda_\chi^2}{m_{ETC}^2}$ coming naturally from the ETC sector (m_{ETC} denotes the relevant ETC scale), a specific model may introduce a small dimensionless parameter into the final results if, for example, CP conservation is only slightly violated in extended technicolor interactions. At energies above Λ_χ but below m_{ETC} , CP violation can be described effectively by a set of ETC-induced, CP-violating four-fermion operators. These operators are added to the usual technicolor lagrangian along with corresponding CP-conserving four-fermion operators. The technicolor interaction itself respects CP symmetry.

In this paper we estimate the effect of these CP-violating four-fermion operators on the CP-odd TGVs, and on further amplitudes induced by the CP-odd TGVs. In the minimal standard model, the CP-odd TGVs are expected to arise via the Kobayashi-Maskawa (KM) mechanism [10] at the three-loop level [11], and thus are suppressed by at least two powers of the weak coupling $\frac{\alpha}{\pi}$ and by the small mixing effect among the three families of quarks. They are thus much too tiny to have experimental signatures in the near future. In technicolor theories, however, assuming maximal CP violation in the ETC sector, our estimates show that these

CP-violating TGVs are much larger than in the minimal standard model, and are comparable to or larger than in other extensions of the standard model [12]. Still they seem unlikely to show up directly in the next generation of high energy collider experiments. It is the indirect low energy effects induced by these CP-odd TGVs, especially the electric-dipole-moment (EDM) of the neutron [13, 14], that will be more accessible to future experiments. We thus include in this paper estimates of the induced EDMs of the neutron (and electron) in technicolor theories.

The paper is organized as follows. In section 2, we write down the CP-odd TGV's, and the CP-violating dimension-four chiral lagrangian operators, along with a table of the C, P and CP transformation properties of all chiral lagrangian operators up to dimension four. The connection between the CP-odd TGV's and the CP-violating chiral lagrangian operators is made. In section 3, we compute the contribution to the CP-odd TGV form factors from a class of CP-violating four-fermion operators induced by single ETC boson exchange. The future high energy experimental detectability of these TGVs is then discussed. The zero momentum limit of the TGVs is studied in connection with the CP-violating electroweak chiral lagrangian operators and the W boson EDM. In section 4, the EDMs of the electron and neutron, induced by the P- and CP-odd $WW\gamma$ effective interaction, are computed and compared to current experimental limits. Some other contributions to the EDMs of the neutron and the electron are found to be less important. We present our conclusions in section 5.

2 CP-Violating TGV's And The Chiral Lagrangian

We begin by writing down the CP-odd WWV ($V = \gamma, Z$) vertices in momentum space, following the notation of Ref. [9]:

$$\begin{aligned}\Gamma_V^{\mu\nu\rho}(p_1, p_2, p) &= if_4^V(p^2)(p^\mu g^{\rho\nu} + p^\nu g^{\rho\mu}) - f_6^V(p^2)\epsilon^{\rho\mu\nu\lambda}p_\lambda \\ &\quad - \frac{f_7^V(p^2)}{\Lambda_\chi^2}(p_1 - p_2)^\rho \epsilon^{\mu\nu\lambda\sigma}p_\lambda(p_1 - p_2)_\sigma,\end{aligned}\quad (2)$$

where p_1 , p_2 and $p = p_1 + p_2$ are the momenta carried by the W^- , W^+ and V bosons respectively. The W bosons are taken to be on-shell. The form factors $f_4^V(p^2)$, $f_6^V(p^2)$ and $f_7^V(p^2)$ could have imaginary parts if p^2 is above physical thresholds. Since we will focus attention on effects from new physics above Λ_χ , we have defined $f_7^V(p^2)$ to be associated with $\frac{1}{\Lambda_\chi^2}$, instead of $\frac{1}{m_W^2}$ as was done in Ref. [9]. We use the convention $\epsilon_{0123} = 1$.

The effective lagrangian for the CP-odd TGV's, which in momentum space corresponds to the $p \rightarrow 0$ limit of Eq. (2), reads [9]:

$$\begin{aligned}\frac{\mathcal{L}_{WWV}^{\text{CP odd}}}{g_{WWV}} &= -g_4^V W_\mu^+ W_\nu^- (\partial^\mu V^\nu + \partial^\nu V^\mu) + i\tilde{\kappa}_V W_\mu^+ W_\nu^- \tilde{V}^{\mu\nu} \\ &\quad + \frac{i\tilde{\lambda}_V}{\Lambda_\chi^2} W_{\mu\nu}^+ W^{-\nu\rho} \tilde{V}^{\rho\mu},\end{aligned}\quad (3)$$

where $W_{\mu\nu}^\pm = \partial_\mu W_\nu^\pm - \partial_\nu W_\mu^\pm$, $V_{\mu\nu} = \partial_\mu V_\nu - \partial_\nu V_\mu$, and $\tilde{V}_{\mu\nu} = \frac{1}{2}\epsilon_{\mu\nu\rho\lambda}V^{\rho\lambda}$. The parameters $g_{WW\gamma}$ and g_{WWZ} are given by $g_{WW\gamma} = -e$ and $g_{WWZ} = -e \cot \theta_W$, where e is the electromagnetic coupling constant, and θ_W is the Weinberg angle. The TGV couplings g_4^V , $\tilde{\kappa}_V$ and $\tilde{\lambda}_V$ are related to the form factors by,

$$\begin{aligned}f_4^V(0) &= g_4^V \\ f_6^V(0) &= \tilde{\kappa}_V - \tilde{\lambda}_V \frac{m_W^2}{\Lambda_\chi^2}\end{aligned}$$

$$f_7^V(0) = -\frac{1}{2}\tilde{\lambda}_V. \quad (4)$$

The electric dipole moment (EDM) d_{W^+} and the magnetic quadrupole moment \tilde{Q}_{W^+} of the W^+ from physics above Λ_χ are directly related to the TGV couplings by $d_{W^+} = \frac{e}{2m_W}(\tilde{\kappa}_\gamma + \tilde{\lambda}_\gamma \frac{m_W^2}{\Lambda_\chi^2})$ and $\tilde{Q}_{W^+} = -\frac{e}{m_W^2}(\tilde{\kappa}_\gamma - \tilde{\lambda}_\gamma \frac{m_W^2}{\Lambda_\chi^2})$ respectively.

The first term in Eq. (3) is P-even and CP-odd. The second and the third terms are both P- and CP-odd. The first two terms are of dimension four and correspond to certain dimension-four terms in the electroweak chiral lagrangian. The last term is of dimension six and is suppressed by a factor of $\mathcal{O}(\frac{p^2}{\Lambda_\chi^2})$ relative to the CP-odd dimension-four terms. It will be neglected in this paper. The g_4^γ term vanishes as a consequence of electromagnetic gauge invariance.

We turn next to the electroweak chiral lagrangian. This is an effective low energy theory valid below the scale Λ_χ . It can be obtained from a more fundamental theory by integrating out the (strongly interacting) heavy degrees of freedom above Λ_χ , and the high energy physics effects are then contained in the coefficients of the chiral lagrangian operators. Sixteen independent operators up to dimension four can be written down [7], after using the equations of motion, for the gauged, electroweak chiral $SU(2)_L \times SU(2)_R$ lagrangian. The leading operator can be obtained from the gauged scalar sector of the minimal standard model by taking the physical Higgs boson mass to infinity. It is given by,

$$\mathcal{L}_0 = \frac{f^2}{4}\text{Tr}[(D_\mu U)^\dagger(D^\mu U)], \quad (5)$$

where $U \equiv \exp(i\vec{\pi} \cdot \vec{\tau}/f)$ and $D_\mu U$ is its electroweak gauge covariant derivative. The τ 's are the three Pauli matrices. Note that $U^\dagger U = 1$ and the dimensions of U and $D_\mu U$ are zero and one respectively. The dimension-two operator \mathcal{L}_0 gives rise to

the W and Z masses with the relation $\frac{m_W^2}{m_Z^2} = \cos^2 \theta_W$. Deviations from this relation can be described by the one other dimension-two operator, \mathcal{L}'_1 of Ref. [4], directly related to the T parameter.

The fourteen dimension-four chiral lagrangian operators are suppressed by a factor of $\frac{1}{\Lambda_\chi^2}$ relative to the dimension-two operators. The coefficients of these dimension-four operators are then naturally of order $\frac{f^2}{\Lambda_\chi^2} = \frac{N_f}{16\pi^2}$ times factors arising from weak-isospin breaking and CP violation (for the CP-violating operators).

The three independent, CP-violating, dimension-four operators of the electroweak chiral lagrangian were designated \mathcal{L}_{12} , \mathcal{L}_{13} , and \mathcal{L}_{14} in Ref. [7]. They are given by,

$$\mathcal{L}_{12} \equiv 2\alpha_{12} g \text{Tr}(T\mathcal{V}_\mu) \text{Tr}(\mathcal{V}_\nu W^{\mu\nu}) \quad (6)$$

$$\mathcal{L}_{13} \equiv \frac{1}{4} \alpha_{13} g g' \epsilon^{\mu\nu\rho\sigma} B_{\mu\nu} \text{Tr}(TW_{\rho\sigma}) \quad (7)$$

$$\mathcal{L}_{14} \equiv \frac{1}{8} \alpha_{14} g^2 \epsilon^{\mu\nu\rho\sigma} \text{Tr}(TW_{\mu\nu}) \text{Tr}(TW_{\rho\sigma}), \quad (8)$$

where $W_{\mu\nu}$, $B_{\mu\nu}$ are the gauge field strengths of $SU(2)_L$ and $U(1)_Y$ respectively, and g and g' are their corresponding gauge couplings. The operators T and \mathcal{V}_μ live in the adjoint representation of $SU(2)_L$ and are singlets under $U(1)_Y$. They are defined by $T \equiv U\tau_3 U^\dagger$ and $\mathcal{V}_\mu \equiv (D_\mu U)U^\dagger$ ². The definitions adopted here for the coefficients α_{12} , α_{13} and α_{14} differ from those in Ref. [7] by the symmetry factors of 2, $\frac{1}{4}$ and $\frac{1}{8}$ respectively, in order to simplify the relations to the TGV couplings below.

It is interesting to observe that the operator \mathcal{L}_{13} is the CP-violating analog of \mathcal{L}_1 of Refs. [4, 7], which is directly related to the weak-isospin symmetric S param-

²The operator field \mathcal{V}_μ used in this paper is the same as denoted by V_μ in Refs. [4, 7], it is used here to avoid confusion with V_μ denoting the γ or Z field.

eter. Similarly \mathcal{L}_{14} is the CP-violating analog of \mathcal{L}_8 , directly related to the weak-isospin-breaking U parameter. The CP-conserving partner of \mathcal{L}_{12} is the custodial-symmetry-breaking operator \mathcal{L}_{11} of Ref. [7], which is the unique dimension-four P- and C-violating but CP-conserving operator $\mathcal{L}_{11} \equiv \alpha_{11} g \epsilon^{\mu\nu\rho\lambda} \text{Tr}(T\mathcal{V}_\mu) \text{Tr}(\mathcal{V}_\nu W_{\rho\lambda})$.

For convenience in relating the chiral lagrangian operators to the electroweak gauge boson vertices, we give in Table 1 the C, P and CP transformation properties of all chiral lagrangian operators up to dimension four in the unitary gauge (setting the Goldstone-boson fields to zero).

	C	P	CP
$\mathcal{L}_0, \mathcal{L}'_1, \mathcal{L}_1 - \mathcal{L}_{10}$	even	even	even
\mathcal{L}_{11}	odd	odd	even
\mathcal{L}_{12}	odd	even	odd
$\mathcal{L}_{13}, \mathcal{L}_{14}$	even	odd	odd

Table 1: The C, P and CP transformation properties of all the sixteen $SU(2)_L \times U(1)_Y$ invariant chiral lagrangian operators up to dimension four in unitary gauge. The operators \mathcal{L}_0 and \mathcal{L}'_1 have dimension two, and the operators \mathcal{L}_1 through \mathcal{L}_{14} have dimension four. All these operators have been listed in Ref. [7].

Note that the sixteen chiral lagrangian operators in general do not have simple transformation properties separately under C and P, though they can be classified as CP-even and CP-odd under the combined CP operation. In unitary gauge, however, they can all be classified as C(P)-even or C(P)-odd, as shown in Table 1. It can be seen from the table that in unitary gauge, both \mathcal{L}_{11} and \mathcal{L}_{12} have unique transformation properties under C, P and CP. Thus, these two operators might be isolated and probed experimentally, if proper observables are chosen and their size is large enough ³.

³Experimental signatures of the CP-conserving operator \mathcal{L}_{11} have been studied in Ref. [16].

In unitary gauge, the CP-even chiral lagrangian operators reduce to two-, three-, and four-gauge-boson vertices, whereas the CP-odd ones generate only three- and four-gauge-boson vertices. There are three independent CP-violating three-gauge-boson vertices, generated by \mathcal{L}_{12} , \mathcal{L}_{13} and \mathcal{L}_{14} . They correspond to terms in the TGV effective lagrangian in Eq. (3). The CP-odd TGV couplings are related to α_{12} , α_{13} and α_{14} by,

$$\tilde{\kappa}_Z = \frac{e^2}{c^2}\alpha_{13} - \frac{e^2}{s^2}\alpha_{14} \quad (9)$$

$$\tilde{\kappa}_\gamma = -\frac{e^2}{s^2}(\alpha_{13} + \alpha_{14}) \quad (10)$$

$$g_4^Z = -\frac{e^2}{s^2 c^2}\alpha_{12} \quad (11)$$

$$g_4^\gamma = 0, \quad (12)$$

where $s^2 = 1 - c^2 \equiv \sin^2 \theta_W$. The on-shell condition for the W bosons has been used in deriving the above relations.

It is noted that there exists only one CP-odd four-gauge-boson vertex at the dimension-four level. It is generated by \mathcal{L}_{12} . (The CP-violating four-gauge-boson effective interaction described by \mathcal{L}_{14} is proportional to $\epsilon_{\mu\nu\rho\sigma}W_1^\mu W_2^\nu W_1^\rho W_2^\sigma$, thus vanishes.) This C-odd and P-even (CP-odd) effective $WWZ\gamma$ vertex is given by,

$$\mathcal{L}_{WWZ\gamma} = i\alpha_{12}\frac{g^3 e}{c}(W^{+\mu}W^{-\nu} - W^{+\nu}W^{-\mu})Z_\mu A_\nu, \quad (13)$$

where A_ν denotes the photon field. This vertex could be interesting experimentally because of its uniqueness. For example, it could be studied at an $e\gamma$ collider via the reaction $e^-\gamma \rightarrow \nu_e W^- Z$, which has been used as a probe for the operator \mathcal{L}_{11} in Ref. [16].

3 CP-Violating Four-Fermion Operators

We now proceed to estimate the above CP-violating TGV parameters in technicolor theories, arising from the underlying ETC interactions. We consider a one-family technicolor model, along with the three quark-lepton generations. The technifermions are taken to belong to the fundamental representation of an $SU(N)_{TC}$ technicolor theory, and transform like ordinary fermions under the standard model gauge group. We assume three different ETC scales, one for each family. The ETC scale associated with the first family is much higher than that associated with the second family, and the ETC scale for the second family is much higher than that for the third. For simplicity, attention will first be restricted to the class of ETC models in which the ETC gauge group commutes with the standard model gauge group. We will describe the CP violation in the ETC interactions in terms of a set of CP-violating, $SU(N)_{TC} \times SU(3)_C \times SU(2)_L \times U(1)_Y$ invariant four-fermion operators induced by single massive ETC gauge boson exchange.

It can be shown that all the single-ETC-boson-induced four-technifermion operators which are $SU(N)_{TC} \times SU(3)_C \times SU(2)_L \times U(1)_Y$ invariant are CP-conserving. It can also be shown that all the CP-violating four-ordinary-fermion operators involve fermions from at least one of the two light families, and are thus suppressed by higher ETC scales. It is only the CP-violating four-fermion operators involving two technifermions and two ordinary fermions from the heaviest family that are suppressed by the lowest ETC scale and therefore have the largest CP-violating effects. The contribution of these four-fermion operators to the CP-odd TGV's turns out to involve two mass insertions of the ordinary fermions. The largest contribution

will therefore come from the CP-violating four-fermion operators consisting of two techniquarks and the (t, b) doublet. There are two of them, given by [17],

$$\mathcal{L}_{4f}^1 \equiv (\bar{q}_L \gamma^\mu Q_L) [\bar{Q}_R \gamma_\mu (a_1 + a_1' \tau_3) q_R] + \text{h.c.} \quad (14)$$

$$\mathcal{L}_{4f}^2 \equiv a_2 (\bar{q}_R \gamma^\mu Q_R) (\bar{Q}_R \gamma_\mu \tau_3 q_R) + \text{h.c.} \quad (15)$$

where q and Q denote the (t, b) doublet and one doublet of techniquarks respectively. The a 's are in general complex, with their magnitudes expected to be of order $\frac{g_{ETC}^2}{m_{ETC}^2}$, where g_{ETC} is the ETC coupling and m_{ETC} denotes the mass of the ETC boson.

The operator \mathcal{L}_{4f}^1 is responsible for the generation of quark masses in technicolor theories, as can be seen by a Fierz rearrangement. When extended to include three families of quarks, it gives rise to the CKM matrix with the Kobayashi-Maskawa (KM) phase [10]. Since CP symmetry is respected by TC interactions, the techniquark condensates will naturally be real. It can then be shown that \mathcal{L}_{4f}^1 with three quark families violates CP only via the KM phase in the CKM matrix appearing in W couplings to the quarks, as well as in four-fermion operators involving both up-type and down-type quarks. All CP-violating effects of \mathcal{L}_{4f}^1 (with three families) will then be suppressed by the small mixing among the three quark-families and will not be considered here.

We turn now to \mathcal{L}_{4f}^2 . After the quarks and techniquarks get their masses, we can rewrite the effective ETC lagrangian in terms of the mass eigenstates of the fermion fields. It can then be seen that \mathcal{L}_{4f}^2 violates CP conservation even with only one family of quarks. Though the CP phase in \mathcal{L}_{4f}^2 could be rotated away by redefining the quark and techniquark fields, it will reappear in other pieces of the effective lagrangian, such as the W couplings to t, b doublet and to techniquarks.

Physical CP-violating effects are independent of this phase rotation.

The operator \mathcal{L}_{4f}^2 contributes to the CP-odd TGV's via the diagrams shown in Fig. 1. The techniquarks in Fig. 1 will of course experience strong TC interactions. As is sometimes done in both QCD and technicolor theories, one could model the strong interactions by employing dynamical mass functions $\Sigma(p)$ for the single-loop of techniquarks and neglecting additional TC interactions. The $\Sigma(p)$'s can be determined by solving Schwinger-Dyson gap equations, with their normalizations fixed by the technipion decay constant f (equivalently the W and Z masses) [18].

After a Fierz rearrangement, it can be seen that the CP-odd piece of \mathcal{L}_{4f}^2 consists of the product of a charge-changing techniquark current and a charge-changing quark current. The CP-odd TGV's are induced by diagrams with the two W bosons attached separately to the quark and techniquark loops, and the V (γ or Z) boson attached to the quark loop, as in Fig. 1. As \mathcal{L}_{4f}^2 consists of two right-handed currents, two mass insertions are needed on each loop. The quark loop integral is then finite. Since the techniquarks develop dynamical masses via the strong TC interactions, with their magnitudes on the order of Λ_χ below the technifermion chiral symmetry breaking scale Λ_χ and falling rapidly with momentum above Λ_χ , the techniquark loop integral will be highly convergent at momentum scales just above Λ_χ .

The diagrams with the V boson attached to the techniquark loop are suppressed by a factor of $\mathcal{O}(\frac{m_t^2}{m_{TF}^2})$ relative to those with the V boson attached to the quark loop as in Fig. 1. This can be understood as follows: in the former case it is the techniquark mass squared m_{TF}^2 that sets the infrared (IR) scale, appearing in the denominator of the technifermion loop integral; while in the latter it is the

top quark mass squared m_t^2 that appears in the denominator of the quark loop integral. Thus we need consider only the diagrams in Fig. 1.

To simplify the computations, we use a momentum independent techniquark mass on the order of the technifermion chiral symmetry breaking scale Λ_χ . This will give a good order-of-magnitude estimate of the techniquark loop integral, because the two techniquark mass insertions in the integral render this constant-mass computation at most logarithmic divergent, cut off at a scale Λ_{CO} just above Λ_χ . As the logarithm is typically of order one, the constant mass estimate is expected to be the same order of magnitude as the dynamical mass calculation.

For the incoming momentum p of the V (γ or Z) boson below Λ_χ , the evaluation of the two-loop diagrams in Fig. 1 for the CP-violating TGV's gives (taking the CKM matrix element $V_{tb} = 1$),

$$f_6^Z(p^2) = \frac{N_C}{16\pi^2} \frac{e^2}{s^2 c^2} \delta \left(\left(-\frac{1}{2} + \frac{2}{3} s^2 \right) I_1^{tbb}(p^2) + \left(\frac{1}{2} - \frac{4}{3} s^2 \right) I_1^{btt}(p^2) \right) \quad (16)$$

$$f_6^\gamma(p^2) = \frac{N_C}{16\pi^2} \frac{e^2}{s^2} \delta \left(-\frac{2}{3} I_1^{tbb}(p^2) + \frac{4}{3} I_1^{btt}(p^2) \right) \quad (17)$$

$$f_4^Z(p^2) = \frac{N_C}{16\pi^2} \frac{e^2}{s^2 c^2} \delta \left(\frac{1}{2} I_2^{tbb}(p^2) + \frac{1}{2} I_2^{btt}(p^2) \right) \quad (18)$$

$$f_4^\gamma(p^2) = 0, \quad (19)$$

where $N_C = 3$ is the number of colors. The p^2 -dependent functions $I_{1,2}^{tbb}(p^2)$ and $I_{1,2}^{btt}(p^2)$ come from the quark loop integration and are given by,

$$\begin{aligned} I_1^{tbb}(p^2) &= \int_0^1 dx \int_0^{1-x} dy \frac{m_t m_b}{P(x, y)} \\ I_2^{tbb}(p^2) &= \int_0^1 dx \int_0^{1-x} dy (2x - 1) \frac{m_t m_b}{P(x, y)}, \end{aligned} \quad (20)$$

where $P(x, y)$ is a polynomial in x and y ,

$$P(x, y) = p^2 xy + m_W^2 (x + y)(1 - x - y) - m_t^2 (1 - x - y) - m_b^2 (x + y). \quad (21)$$

The functions $I_1^{btt}(p^2)$ and $I_2^{btt}(p^2)$ can be obtained by exchanging m_t and m_b in the above expressions for $I_1^{tbb}(p^2)$ and $I_2^{tbb}(p^2)$ respectively. The p^2 -independent δ parameter arises from the techniquark loop integration and is a measure of CP violation at momentum scales just below Λ_χ .

In the constant mass ($m_{TF} \sim \mathcal{O}(\Lambda_\chi)$) approximation, one is led to the simple expression for δ ,

$$\delta \simeq \text{Im} a_2 N_{TC} \frac{m_{TF}^2}{4\pi^2} \ln \frac{\Lambda_{CO}^2}{m_{TF}^2}. \quad (22)$$

Recall that a_2 is the coefficient of the CP-violating four-fermion operator \mathcal{L}_{4f}^2 in Eq.(15), and that the CP-odd piece of \mathcal{L}_{4f}^2 is proportional to the imaginary part of a_2 (i.e. $\text{Im} a_2$). It is worth noting that this techniquark loop computation can be viewed as generating the CP-violating, dimension-four chiral lagrangian operator [17],

$$i\delta' \bar{q}_R \tau_3 U^\dagger (D_\mu U) \gamma^\mu q_R + \text{h.c.}, \quad (23)$$

where $q = (t, b)$ and $\delta = 2\text{Im}\delta'$. The remaining part of the computation leading to Eqs. (16–19) then takes place in the low energy chiral lagrangian framework. Considering that the size of δ estimated later could be of order 10^{-2} , this operator suggests the possibility of large CP-violating effects in the decay $t \rightarrow W^+ + b$.

For numerical evaluations, we take $p^2 = (200\text{GeV})^2$, the typical energy at which the LEP(200) collider operates, and $m_b \simeq 5 \text{ GeV}$. Since p^2 is then well above $b\bar{b}$ threshold, the functions $I_{1,2}^{tbb}$ will have an imaginary part as well as a real part. Depending on the top quark mass and the parameter δ , the results of Table 2 are obtained.

m_t (GeV)	$f_6^Z (\times 10^{-4} \cdot \delta)$	$f_6^\gamma (\times 10^{-4} \cdot \delta)$	$f_4^Z (\times 10^{-4} \cdot \delta)$	f_4^γ
130	$-1.2 + 2.6 i$	$-6.7 + 3.8 i$	$2.3 + 0.8 i$	0
160	$-0.4 + 2.4 i$	$-3.9 + 3.5 i$	$1.8 + 0.6 i$	0
175	$-0.2 + 2.3 i$	$-3.1 + 3.4 i$	$1.6 + 0.5 i$	0
200	$0.1 + 2.1 i$	$-2.2 + 3.2 i$	$1.4 + 0.4 i$	0

Table 2: Size of the CP-violating TGV form factors from the four-fermion operator \mathcal{L}_{4f}^2 in a generic ETC model. The numbers in the table are computed at $p^2 = (200\text{GeV})^2$ and should be multiplied by $10^{-4}\delta$.

To determine the size of these CP-violating TGVs, we next estimate δ . The ETC scale associated with the top quark must be in the range from several TeV to 10 TeV to be consistent with a top mass of 150 GeV or above [1, 2]. For our estimate m_{ETC} will be taken to be 5 TeV. We will assume that the ETC interactions are relatively strong, with $g_{ETC}^2 \sim \frac{4\pi^2}{N_{TC}}$ ⁴. In the absence of a specific ETC model of CP violation, there is no obvious reason for CP-violating interactions to be suppressed in the ETC sector. In this paper, we will assume maximal CP violation in extended technicolor interactions. As a consequence, the CP-violating four-fermion operator \mathcal{L}_{4f}^2 will have approximately equal strengths in its CP-even piece and CP-odd piece, namely, $|\text{Im}a_2| \simeq |\text{Re}a_2| \simeq \frac{1}{4} \frac{g_{ETC}^2}{m_{ETC}^2}$ ⁵. As the constant techniquark mass is of order 1 TeV, the size of the CP-violating parameter δ from new physics above Λ_χ can be

⁴This is roughly the critical strength for the four-fermion interactions to trigger chiral symmetry breaking in an asymptotically free gauge theory. See Ref. [19] for details.

⁵The CP violation observed in the neutral Kaon system will not be upset by maximal CP violation in \mathcal{L}_{4f}^2 because of the small mixing between the third and the first two families.

estimated as,

$$\begin{aligned}
\delta &\simeq \text{Im} a_2 N_{TC} \frac{m_{TF}^2}{4\pi^2} \ln \frac{\Lambda_{CO}^2}{m_{TF}^2} \\
&\simeq \frac{g_{ETC}^2}{4m_{ETC}^2} N_{TC} \frac{m_{TF}^2}{4\pi^2} \ln \frac{\Lambda_{CO}^2}{m_{TF}^2} \\
&\simeq \frac{4\pi^2/N_{TC}}{4m_{ETC}^2} N_{TC} \frac{m_{TF}^2}{4\pi^2} \ln \frac{\Lambda_{CO}^2}{m_{TF}^2} \\
&\simeq \frac{1}{4} \frac{m_{TF}^2}{m_{ETC}^2} \cdot \mathcal{O}(1) \\
&\simeq 0.01
\end{aligned} \tag{24}$$

up to an overall minus sign. Recall that Λ_{CO} , m_{TF} and Λ_χ are of the same order of magnitude.

The CP-violating TGV form factors, at $p^2 = (200\text{GeV})^2$ and with the top quark mass 175 GeV, can then be estimated (up to an overall minus sign),

$$\begin{aligned}
f_6^Z((200\text{GeV})^2) &\simeq (-0.2 + 2.3i) \times 10^{-6} \\
f_6^\gamma((200\text{GeV})^2) &\simeq (-3.1 + 3.4i) \times 10^{-6} \\
f_4^Z((200\text{GeV})^2) &\simeq (1.6 + 0.5i) \times 10^{-6} \\
f_4^\gamma &= 0
\end{aligned} \tag{25}$$

Note that the form factors are complex. They also vary with p^2 , though the order of magnitude remains unchanged for p^2 below Λ_χ^2 . The above size of the CP-odd TGV form factors in technicolor theories is comparable to or larger than estimates made in other extensions of the standard model [12].

These form factors can be studied at $p\bar{p}$ colliders and the next generation of e^+e^- colliders via, for example, measurements of CP-odd asymmetries of the two W -decays in the purely leptonic, purely hadronic and mixed channels [9, 15]. The

expected precision of the TGV form factors attainable at LEP(200) is no better than $\mathcal{O}(10^{-2})$. It thus seems hopeless for the effects of these CP-violating TGVs to show up there in $e^+e^- \rightarrow W^+W^-$. Even in other high energy processes including $e\gamma \rightarrow W\nu$ and $\gamma\gamma \rightarrow WW$ [20], where it has been suggested that a limit of $\mathcal{O}(10^{-3})$ on the form factors $\text{Im}f_6^V$ can be reached at energies of about 1 TeV, direct observation of the CP-violating TGVs seems unlikely. The most stringent bounds currently available on the CP-odd TGVs come from measurements of low energy quantities, especially the EDM of the neutron, to which we turn in the next section.

The $p \rightarrow 0$ limit of the TGVs is relevant for low energy quantities like the EDM of the W boson. It also makes direct contact with the chiral lagrangian coefficients α_{12} , α_{13} and α_{14} . From Eqs. (9–12) and Eqs. (16–19), we have for on-shell W bosons (up to an overall sign associated with δ)

$$\begin{aligned}\alpha_{12} &= \frac{N_C}{16\pi^2} \delta \left(-\frac{1}{2}I_2^{tbb}(0) - \frac{1}{2}I_2^{btt}(0) \right) \simeq -3.1 \times 10^{-6} \\ \alpha_{13} &= \frac{N_C}{16\pi^2} \delta \left(\frac{1}{6}I_1^{tbb}(0) - \frac{5}{6}I_1^{btt}(0) \right) \simeq -1.6 \times 10^{-6} \\ \alpha_{14} &= \frac{N_C}{16\pi^2} \delta \left(\frac{1}{2}I_1^{tbb}(0) - \frac{1}{2}I_1^{btt}(0) \right) \simeq -1.7 \times 10^{-5}.\end{aligned}\tag{26}$$

The numbers are for a top quark mass of 175 GeV, with maximal CP violation in the ETC interactions assumed. Note that the enhancement of α_{14} relative to α_{12} and α_{13} arises from the presence of an infrared logarithm $\ln \frac{m_b^2}{m_W^2}$ in the integral function $I_1^{tbb}(0)$ but not in $I_1^{btt}(0)$ and $I_2^{tbb}(0) = I_2^{btt}(0)$, and the partial cancelation between the two terms in the expression of α_{13} in Eq. (26). The appearance of the IR logarithm can be seen by a simple power counting analysis, and it occurs only in the limit $p \rightarrow 0$. Of course, the four integral functions have the same chirality suppression factor $\frac{m_t m_b}{m_W^2}$ so that they go to zero in the limit of vanishing m_b . Apart

from the factor $\frac{1}{16\pi^2} \sim \frac{f^2}{\Lambda_\chi^2}$, these coefficients contain the expected CP-violating suppression factor $\delta \simeq \text{Im} a_2 N_{TC} \frac{m_{TF}^2}{4\pi^2} \ln \frac{\Lambda_{GQ}^2}{m_{TF}^2} \simeq \frac{m_{TF}^2}{4m_{ETC}^2}$ arising from integrating out heavy degrees of freedom above Λ_χ . This δ factor is of course absent in the CP-conserving chiral lagrangian operators.

The TGV parameters $\tilde{\kappa}_\gamma$, $\tilde{\kappa}_Z$ and g_4^Z are related to α_{12} , α_{13} and α_{14} by Eqs. (9–12). The P- and CP-odd TGV couplings $\tilde{\kappa}_\gamma$ and $\tilde{\kappa}_Z$ directly measure the electric-dipole-moment of the W boson $d_{W^+} = \frac{e}{2m_W} \tilde{\kappa}_\gamma$, and the analogous weak-dipole-moment of the W boson respectively. These TGV couplings can readily be obtained from Eq. (26) (up to an overall sign):

$$\tilde{\kappa}_Z \simeq 6.9 \times 10^{-6}, \quad \tilde{\kappa}_\gamma \simeq 7.8 \times 10^{-6}, \quad g_4^Z \simeq 1.7 \times 10^{-6}, \quad (27)$$

where the numbers are for a top quark mass of 175 GeV and maximal CP violation in the ETC sector. The W boson EDM, $d_{W^+} = \frac{e}{2m_W} \tilde{\kappa}_\gamma$, is then given by,

$$\begin{aligned} d_{W^+} &= \frac{3}{4\pi^2} e \sqrt{2} G_F m_W \delta \left(\frac{2}{3} I_1^{btt}(0) - \frac{1}{3} I_1^{tbb}(0) \right) \\ &\simeq 9.6 \times 10^{-20} \delta \text{ e cm} \simeq \pm 1 \times 10^{-21} \text{ e cm}. \end{aligned} \quad (28)$$

This is much larger than the standard model prediction, a three-loop effect less than 10^{-38} e cm , and is comparable to or larger than its estimates in other models of CP violation [11].

4 The EDMs of the Neutron and the Electron

There exist various indirect low energy experimental bounds on the CP-violating TGVs [13, 14]. The most stringent constraint of this sort comes from the neutron EDM [13], which can be induced by the P- and CP-odd $WW\gamma$ effective interaction.

Describing the strength of this $WW\gamma$ vertex by $\tilde{\kappa}_\gamma$, the computation of the induced neutron EDM d_n^γ contains an ultraviolet logarithmic divergence. This means that the neutron EDM is described by a separate (dimension-five) term in the effective chiral lagrangian — extended to include quark fields — and that in the absence of a high energy theory there is in principle no connection between the two low energy parameters $\tilde{\kappa}_\gamma$ and d_n^γ .

One approach to the logarithmic divergence of the neutron EDM in the absence of a high energy theory has been to regulate the high energy physics responsible for the low energy P- and CP-odd $WW\gamma$ interaction by assigning a form factor to the $WW\gamma$ vertex [13]. The form factor was taken to be approximately constant ($\sim \tilde{\kappa}_\gamma$) up to new physics scale $\Lambda \gg m_W$, and falling rapidly for momentum above Λ . Then the induced neutron EDM was found to be [13],

$$\frac{d_n^\gamma}{e} = -\frac{1}{16\pi^2} g_A \xi \sqrt{2} G_F m_N \tilde{\kappa}_\gamma \left(\ln \frac{\Lambda^2}{m_W^2} + \mathcal{O}(1) \right), \quad (29)$$

where $g_A = 1.26$ is the axial-vector coupling constant measured in neutron β -decay, $\xi \simeq 0.2$ is the average fraction of the neutron momentum carried by a valence quark, G_F is the Fermi constant and m_N is the mass of the nucleon. Assuming $|\ln \frac{\Lambda^2}{m_W^2} + \mathcal{O}(1)| > 1$ and requiring that the induced neutron EDM be less than its direct experimental bound $|d_n^\gamma| \leq 1.2 \times 10^{-25} e \text{ cm}$ [21], it follows that

$$|\tilde{\kappa}_\gamma| < 2 \times 10^{-4}. \quad (30)$$

Our low energy estimate, Eq. (27), lies well within this bound, indicating that maximal CP violation in the extended technicolor interactions is allowed by current experiments.

With a high energy theory such as technicolor in hand, a direct connection

between $\tilde{\kappa}_\gamma$ and d_n^γ can in principle be established. By starting with the CP-violating four-fermion operators arising from ETC interactions, an estimate can be made of the $WW\gamma$ form factor and the neutron (and electron) EDM. As the CP-violating effects from \mathcal{L}_{4f}^1 (with three families) are suppressed by the small mixing among the three quark families, the dominant contribution to the $WW\gamma$ form factor and the EDMs of the neutron and electron will come from the operator \mathcal{L}_{4f}^2 of Eq. (15).

A fermionic EDM can be induced from the P- and CP-odd $WW\gamma$ vertex by connecting the two W boson lines to the fermion line. The $WW\gamma$ form factor is generated from \mathcal{L}_{4f}^2 via the diagrams in Fig. 1 for arbitrary W boson momentum. As will be shown shortly, the induced fermionic EDM is dominated by W boson momenta on the order of m_t and below, and the diagrams with the quark and the techniquark loops interchanged are suppressed by $\mathcal{O}(\frac{m_t^2}{m_{TF}^2})$ relative to the diagrams shown in Fig. 1. They will thus not be considered here. The momentum flows of the effective $WW\gamma$ vertex are shown in Fig. 2.

We are now interested in the limit $p \rightarrow 0$, where p denotes the incoming momentum of the photon. Keeping terms up to quadratic in p , the momentum space structure of the $WW\gamma$ vertex is,

$$\Gamma_{\lambda\mu\nu}(k, p) \equiv -\epsilon_{\lambda\mu\nu\alpha} p^\alpha \frac{1}{8\pi^2} \frac{e^2}{s^2} \delta \cdot (I_0(k^2) + k \cdot p I_1(k^2)), \quad (31)$$

where k and $k + p$ are the incoming and outgoing momenta of the W_ν^- and W_μ^- bosons respectively, and δ arises from integrating out the techniquarks and is given by the k^2 independent expression of Eq. (22) for $|k^2| \ll m_{TF}^2$. The CKM matrix element V_{tb} has been set to unity. The integral functions $I_0(k^2)$ and $I_1(k^2)$ come

from the quark loop integral and are defined as,

$$\begin{aligned} I_0(k^2) &= \int_0^1 dx \frac{m_t m_b (3x - 2)}{-k^2 x(1-x) + m_t^2(1-x) + m_b^2 x} \\ I_1(k^2) &= \int_0^1 dx \frac{m_t m_b (3x - 2)x(1-x)}{[-k^2 x(1-x) + m_t^2(1-x) + m_b^2 x]^2}. \end{aligned} \quad (32)$$

In Eq. (31), the form factor is defined for the W bosons either on- or off-shell and in the limit $p \rightarrow 0$. Requiring the W bosons to be on-shell, Eq. (31) reduces to the $f_6^\gamma(p^2)$ term of Eq. (2) in the limit of small photon momentum.

It can be seen from Eq. (32) that the $WW\gamma$ vertex falls as $\frac{1}{-k^2}$ (up to a logarithm) for $-k^2$ above roughly m_t^2 . Therefore the induced fermionic EDM converges rapidly when the W boson loop momentum increases above m_t , and the dominant contribution to the fermion EDM is expected to come from the momentum range $-k^2 \ll m_{TF}^2$, which justifies the k^2 -independent expression for δ given by Eq. (22).

We now estimate the EDM of the electron. Keeping terms linear in the electron mass m_e , a unitary-gauge calculation of the diagram in Fig. 3 gives,

$$\frac{d_e^\gamma}{e} = -\left(\frac{1}{16\pi^2}\right)^2 \frac{e^2}{s^2} 2\sqrt{2} G_F m_e \delta \cdot h\left(\frac{m_t^2}{m_W^2}, \frac{m_b^2}{m_W^2}\right), \quad (33)$$

where G_F is the Fermi constant, and the function $h(t, b)$ is given by,

$$h(t, b) = \sqrt{tb} \int_0^1 dx \frac{3x - 2}{t(1-x) + bx - x(1-x)} \ln \frac{t(1-x) + bx}{x(1-x)}. \quad (34)$$

For $m_t = 175\text{GeV}$ and $m_b \simeq 5\text{GeV}$, $h(\frac{m_t^2}{m_W^2}, \frac{m_b^2}{m_W^2}) \simeq 0.24$. Assuming maximal CP violation in the ETC sector (taking $|\delta| \simeq 0.01$ from Eq. (24)), the EDM of the electron is estimated to be (up to an overall minus sign associated with δ),

$$d_e^\gamma \simeq -1.2 \times 10^{-27} \delta \text{ e cm} \simeq -1 \times 10^{-29} \text{ e cm}. \quad (35)$$

It is again worth noting that the computation of the electron EDM can be viewed as a two-step process. The first step consists of integrating out techniquarks above the technicolor chiral symmetry breaking scale, thereby generating the operator of Eq. (23). The second step is doing a two-loop calculation in the electroweak chiral lagrangian framework.

The technicolor result for d_e^γ (Eq. 35) is to be compared with the standard model prediction of less than $10^{-37} e \text{ cm}$ [23], arising at the four-loop level and further suppressed by the small mixing effect among the three families of quarks. In technicolor theories, the dominant contribution to the electron EDM involves only the third family of quarks and the heavy techniquarks, and it arises at two loops in the weak coupling expansion. The current experimental limit on the electron EDM, $d_e^\gamma = (-2.7 \pm 8.3) \times 10^{-27} e \text{ cm}$ [22], is about three orders of magnitudes larger than the estimate in technicolor theories. However, there is a good prospect for significant improvement over the present experimental limit using the YbF molecule [24].

We next turn to the neutron EDM. Keeping terms linear in the light quark masses, and neglecting the W couplings connecting the first and the third families of quarks, the EDM of the u or d quark can be similarly computed from the diagram in Fig. 3. The result is,

$$\frac{d_f^\gamma}{e} = I_3^f \left(\frac{1}{16\pi^2} \right)^2 \frac{e^2}{s^2} 4\sqrt{2} G_F m_f \delta \cdot h\left(\frac{m_t^2}{m_W^2}, \frac{m_b^2}{m_W^2}\right), \quad (36)$$

where $f = u$ or d , and $I_3^u = \frac{1}{2}$ and $I_3^d = -\frac{1}{2}$ are the third components of the weak isospin of the u and d quarks.

As the neutron EDM is measured below the hadronic scale where the chiral symmetry breaking effects of the light quarks become important, the constituent

quark masses of $m_u \simeq m_d \simeq \frac{m_N}{3}$ (m_N being the nucleon mass) are appropriate for use in Eq. (36). By use of the nonrelativistic quark model relation, $d_n^\gamma = \frac{4}{3}d_d^\gamma - \frac{1}{3}d_u^\gamma$, we then get [25],

$$\frac{d_n^\gamma}{e} = -\frac{10}{9} \left(\frac{1}{16\pi^2}\right)^2 \frac{e^2}{s^2} \sqrt{2} G_F m_N \delta \cdot h\left(\frac{m_t^2}{m_W^2}, \frac{m_b^2}{m_W^2}\right). \quad (37)$$

For numerical evaluation, we take $m_t = 175\text{GeV}$ and $m_b \simeq 5\text{GeV}$, and again assume maximal CP violation in the ETC interactions ($|\delta| \simeq 0.01$). The neutron EDM is then estimated to be (up to an overall sign),

$$d_n^\gamma \simeq -1.2 \times 10^{-24} \delta \text{ e cm} \simeq -1 \times 10^{-26} \text{ e cm}. \quad (38)$$

In the standard model, by contrast, the neutron EDM appears at the three-loop-level, and is estimated to be less than 10^{-31} e cm [26], far below the current experimental bound of $|d_n^\gamma| < 1.2 \times 10^{-25} \text{ e cm}$ [21]. Since our estimate of the neutron EDM is near the current experimental bound, further experimental improvement [27] on the limit of the neutron EDM could help to reveal the precise nature of CP violation in extended technicolor interactions.

It is interesting to note that by using the value of $\tilde{\kappa}_\gamma$ of Eq. (27) to describe the strength of the P- and CP-odd $WW\gamma$ vertex and computing the induced fermion EDM with an ultraviolet cutoff Λ , as in the previous section, the size of the resulting neutron and electron EDMs roughly agrees with our dynamical calculations of Eqs. (35) and (38) when simply setting the logarithm $\ln \frac{\Lambda^2}{m_W^2}$ to 1. This can be understood easily if we recall that in the dynamical computation, the cutoff Λ should be replaced by roughly m_t , as can be seen from the form factor of Eqs. (31) and (32), and that $\ln \frac{m_t^2}{m_W^2} \simeq 1.6$ for a top quark mass of 175 GeV.

To conclude this section, we note that the CP-violating operator of Eq. (23) can be extended to include the three known families of quarks and leptons, with the leptonic operators being generated by integrating out the technileptons. A fermion EDM can then be induced by these CP-violating operators at one-loop in the weak-coupling expansion (see Fig. 4). For the EDMs of the neutron and the electron, however, the external fermions of Fig. 4 belong to the first family, and the corresponding ETC scale is about 1000 TeV. As this scale is much higher than the ETC scale for the third family, the neutron and electron EDMs induced by the diagrams of Fig. 4 will be smaller than those induced by the P- and CP-odd $WW\gamma$ vertex of Fig. 3.

The neutron EDM is induced by both types of diagrams in Fig. 4, with the external fermion denoting a u or d quark. For the internal fermions being the first family of quarks, and using the nonrelativistic quark model relation $d_n^\gamma = \frac{4}{3}d_d^\gamma - \frac{1}{3}d_u^\gamma$, we find,

$$\left. \frac{d_n^\gamma}{e} \right|_{\text{Fig. 4}} = \frac{4}{9} \frac{\sqrt{2}G_F}{4\pi^2} V_{ud} (5m_u - m_d) \delta_1, \quad (39)$$

where δ_1 characterizes the strength of the CP-violating operator Eq. (23) for the first family of quarks. Taking the ETC scale for the first family to be 1000 TeV, and assuming maximal CP violation in the ETC interactions, δ_1 can be estimated by integrating out the techniquarks. It is of order 10^{-7} or less. Using the constituent quark mass $m_u \simeq m_d \simeq \frac{m_N}{3}$, the induced neutron EDM is (up to an overall sign)

$$d_n^\gamma|_{\text{Fig. 4}} \sim 10^{-28} - 10^{-27} \text{ e cm.} \quad (40)$$

This is one to two orders of magnitudes smaller than the P- and CP-odd $WW\gamma$ -vertex-induced EDM of Eq. (38). It can be further shown that if the internal

quarks belong to the second and third families, the induced neutron EDM from Fig. 4 is either in range $10^{-28} - 10^{-27} e \text{ cm}$ or smaller, assuming all the relevant CP-violating effective $W \bar{f}_1 f_2$ vertices have the same strengths. Therefore these one-loop contributions to the neutron EDM can be safely neglected.

The electron EDM is generated only by the first diagram in Fig. 4. A straightforward computation gives,

$$\left. \frac{d_e^\gamma}{e} \right|_{\text{Fig. 4}} = \frac{\sqrt{2} G_F}{4\pi^2} m_{\nu_e} \delta_e, \quad (41)$$

where m_{ν_e} is the mass of the electron neutrino and δ_e characterizes the strength of the leptonic version of the CP-violating operator of Eq. (23) for the first family of leptons, generated by integrating out the technielectron and technineutrino. As the mass of a Dirac-type electron neutrino is experimentally bounded to be at most several eV, its contribution to the electron EDM can be neglected.

A sizable value for m_{ν_e} is possible via the see-saw mechanism if the right-handed neutrino gets a large Majorana mass. In this case, m_{ν_e} will be the off-diagonal Dirac mass term in the Majorana neutrino mass matrix, and it could be assumed to have a value on the order of the mass of its charged lepton partner. For our estimate, the ETC scale is taken to be 1000 TeV, and the technielectron and the technineutrino masses are taken to be 400 GeV and 200 GeV respectively. Then $\delta_e \sim \mathcal{O}(10^{-8})$ with maximal CP violation in the ETC interactions. Assuming $m_{\nu_e} \sim 1 \text{ MeV}$, the induced electron EDM is then (up to an overall sign)

$$d_e^\gamma|_{\text{Fig. 4}} \sim 10^{-31} e \text{ cm}. \quad (42)$$

This is two orders of magnitudes smaller than the $WW\gamma$ -vertex-induced value of Eq. (35). Therefore we can neglect these one-loop contributions to the electron

EDM.

So far we have restricted attention to the CP-violating four-fermion operators induced by exchanging color- and electroweak- neutral ETC bosons. CP-violating effects from an ETC sector which has ETC bosons carrying nontrivial standard model quantum numbers can and should be estimated. For example, in a complete ETC theory, quarks and leptons as well as techniquarks and technileptons can be unified at higher energies via the exchange of Pati-Salam colored gauge bosons [28, 2], and new CP-violating electroweak invariant four-fermion operators could be generated. Most notable are the operators involving two techniquarks and two technileptons, where there are no mass-insertion suppressions when generating the CP-odd TGVs. These four-technifermion operators, however, are suppressed by the masses of the Pati-Salam bosons which could be above 1000 TeV [2], and their CP-violating effects can thus be neglected.

5 Conclusion

In this paper, the CP-odd $WW\gamma$ and WWZ vertices have been examined in technicolor theories. This has been done using effective four-fermion interactions to describe the high energy ETC sector responsible for the weak CP violation. The technicolor interactions respect the CP symmetry. The dominant contribution to the CP-odd TGVs comes from the operator \mathcal{L}_{4f}^2 (Eq. (15)), which is induced by color- and electroweak- neutral ETC boson exchange. This CP-violating four-fermion operator consists of a techniquark doublet and the (t,b) doublet.

The size of the CP-odd $WW\gamma$ and WWZ form factors in technicolor theo-

ries is estimated to be of order 10^{-6} at center of mass energy 200GeV (Eq. (25)), assuming that CP symmetry is maximally violated in the ETC interactions. This is much larger than the minimal standard model prediction, and is comparable to or larger than estimates made in other extensions of the standard model [12]. Unfortunately the precision on the CP-violating TGV form factors attainable at LEP(200) is at best of $\mathcal{O}(10^{-2})$, and it is impossible for these CP-violating effects to show up in the next generation of e^+e^- experiments. Even in high energy processes like $e\gamma \rightarrow W\nu$ and $\gamma\gamma \rightarrow WW$ at about 1 TeV, where the limit on the TGVs could reach $\mathcal{O}(10^{-3})$ [20], direct observation of these CP-violating vertices still seems unlikely.

The coefficients of the three CP-violating, dimension-four electroweak chiral lagrangian operators, defined in the $p \rightarrow 0$ limit, are estimated in technicolor theories to be of order $10^{-6} - 10^{-5}$ (Eq. (26)), about three orders of magnitudes smaller than the CP-conserving, dimension-four (custodial symmetry preserving) ones estimated in Ref. [7]. This can be understood as follows. The dimension-four CP-conserving (custodial symmetry preserving) chiral lagrangian operators are generated by integrating out the strongly interacting technifermions, and are independent of the higher scale ETC interactions. Their size is therefore of order $\frac{f^2}{\Lambda_\chi^2} \simeq \frac{N_f}{16\pi^2}$. The CP-violating chiral lagrangian operators, however, originate from the high energy (CP-nonconserving) ETC interactions, and are naturally suppressed by $\frac{\Lambda_\chi^2}{m_{ETC}^2}$ relative to the CP-conserving operators. In the types of ETC models considered in this paper, there is in addition the chirality suppression factor $\frac{m_t m_b}{m_W^2}$ in the three CP-violating chiral lagrangian operators. The connection between the CP-odd TGV couplings and CP-violating chiral lagrangian operators is made in Eqs. (9-12).

Severe constraints on the CP-odd TGVs can be obtained from low energy

quantities like the electric- and weak-dipole moments of the quarks and leptons [13, 14]. Among them the neutron EDM supplies the most stringent bound. Consistency between the current experimental limit on the neutron EDM and its induced value from a P- and CP-odd $WW\gamma$ vertex requires $|\tilde{\kappa}_\gamma| < 2 \times 10^{-4}$. In technicolor theories, the chiral lagrangian parameter $\tilde{\kappa}_\gamma$ is estimated to be $|\tilde{\kappa}_\gamma| \sim \mathcal{O}(10^{-5})$. This corresponds to an EDM of the W boson of $\mathcal{O}(10^{-21}) e \text{ cm}$, and lies comfortably within the above indirect experimental bound. The W EDM in technicolor theories is much larger than the standard model expectation $< 10^{-38} e \text{ cm}$ [11], and is comparable to or larger than its size in other models of CP violation.

The P- and CP-odd $WW\gamma$ vertex for off-shell W bosons can be computed in technicolor theories, and used to estimate the EDMs of the neutron and the electron. The $WW\gamma$ vertex falls like $\frac{1}{k^2}$ for the W boson momentum k above m_t , and a finite expression can be written down for the induced fermion EDM. The EDM of the electron is estimated to be as large as $\mathcal{O}(10^{-29}) e \text{ cm}$, three orders of magnitudes below the present experimental limit. Significant improvement over the current experimental limit on the electron EDM is expected in the near future using new experimental methods [24]. The neutron EDM in technicolor theories can be as large as $\mathcal{O}(10^{-26}) e \text{ cm}$, not far from the current experimental bound of less than $1.2 \times 10^{-25} e \text{ cm}$. Future experimental improvements [27] on the limit of the neutron EDM could help to reveal the precise nature of CP violation in extended technicolor interactions.

As the ETC scale for the first fermion family is two orders of magnitudes higher than for the third family, the induced EDMs of the neutron and electron from one-loop diagrams of Fig. 4 turn out to be one to two orders of magnitudes

smaller than induced from the P- and CP-odd $WW\gamma$ vertex (Fig. 3) — a two-loop effect in the weak coupling expansion. Because of the relatively low ETC scale associated with the third family of quarks, it is also suggested that potentially large CP-violating effects could be observed in the decay $t \rightarrow b + W^+$.

Acknowledgments

We like to thank W. Marciano and S. Selipsky for helpful conversations, and J. Liu for pointing out to us Ref. [11]. This work is supported by a DOE grant DE-AC02ERU3075.

References

- [1] M. Einhorn and D. Nash, Nucl. Phys. **B371** (1992) 32;
S. King and S. Mannan, Nucl. Phys. **B369** (1992) 119;
L. Randall and R. Sundrum, Phys. Lett. **B312** (1993) 148.
- [2] T. Appelquist and J. Terning, Yale University preprint, YCTP-P21-93, and
Boston University Preprint, BUHEP-93-23,1993, to be published in Phys.
Rev. **D**.
- [3] E. Eichten, K. Lane and J. Preskill, Phys. Rev. Lett. **45** (1980) 225;
A. Buras, S. Dawson and A. Schellekens, Phys. Rev. **D27** (1983) 1171.
- [4] T. Appelquist and C. Bernard, Phys. Rev. **D22** (1980) 200;
A. Longhitano, Phys. Rev. **D22** (1980) 1166; Nucl. Phys. **B188**, (1981) 118;
T. Appelquist, in “Gauge theories and experiments at high energies”, ed. by

- K. Brower and D. Sutherland, Scottish University Summer School in Physics, St. Andrews (1980).
- [5] For recent reviews on electroweak effective lagrangian, see, for example, F. Feruglio, *Int. Jour. of Mod. Phys.* **A8** (1993) 4937; C. Arzt, M. Einhorn and J. Wudka, University of Michigan preprint UM-TH-94-15, UCRHEP-125, CALT-68-1932 (1994); J. Wudka, University of California preprint, UCRHEP-T121 (1994).
- [6] M. Soldate and R. Sundrum, *Nucl. Phys.* **B340** (1990) 1;
R. Chivukula, M. Dugan and M. Golden, *Phys. Rev.* **D47** (1993) 2930;
T. Appelquist and J. Terning, *Phys. Rev.* **D47** (1993) 3075.
- [7] T. Appelquist and G.-H. Wu, *Phys. Rev.* **D48** (1993) 3235.
- [8] M. Peskin and T. Takeuchi, *Phys. Rev. Lett.* **65** (1990) 964; *Phys. Rev.* **D46** (1992) 381.
- [9] K. Hagiwara, R. Peccei, D. Zeppenfeld and K. Hikasa, *Nucl. Phys.* **B282** (1987) 253.
- [10] M. Kobayashi and T. Maskawa, *Prog. Theor. Phys.* **49** (1973) 652.
- [11] D. Chang, W.Y. Keung and J. Liu, *Nucl. Phys.* **B355** (1991) 295;
M. Pospelov, and I. Khriplovich, *Sov. J. Nucl. Phys.* **53** (1991) 638.
- [12] See, for example, X. He, J. Ma and B. McKellar, *Phys. Lett.* **B304** (1993) 285.
- [13] W. Marciano and A. Queijeiro, *Phys. Rev.* **D33** (1986) 3449. See also S. Barr and W. Marciano, in “CP violation”, edited by C. Jarlskog (World Scientific, Singapore, 1989)

- [14] A. De Rújula, M. Gavela, O. Pène and F. Vegas, Nucl. Phys. **B357**, (1991) 311.
- [15] For a recent discussion, see D. Chang, W.Y. Keung and I. Phillips, Phys. Rev. **D48** (1993) 4045, and references therein.
- [16] S. Dawson and G. Valencia, Phys. Rev. **D49** (1994) 2188;
K. Cheung, S. Dawson, T. Han and G. Valencia, UCD-94-6 and NUHEP-TH-94-2, March 1994.
- [17] T. Appelquist, M. Bowick, E. Cohler and A. Hauser, Phys. Rev. **D31** (1985) 1676.
- [18] H. Pagels and S. Stokar, Phys. Rev. **D20** (1979) 2947;
B. Holdom, J. Terning and K. Verbeek, Phys. Lett. **B232** (1989) 351.
- [19] T. Appelquist, M. Soldate, T. Takeuchi and L.C.R. Wijewardhana, in “TeV Physics”, proceedings of the 12th Johns Hopkins Workshop on Current Problems in Particle Theory, Baltimore, Maryland, 1988, edited by G. Domokos and S. Kovesi-Domokos (World Scientific, Singapore, 1989);
K. Kondo, H. Mino and K. Yamawaki, Phys. Rev. **D39** (1989) 2430;
M. Inoue, T. Muta and T. Ochiuni, Mod. Phys. Lett. **A4** (1989) 605.
- [20] A. Queijeiro, Phys. Lett. **B193** (1987) 354;
G. Bélanger and G. Couture, Phys. Rev. **D49** (1994) 5720.
- [21] K.F. Smith *et al.*, Phys. Lett, **B234** (1990) 191;
I.S. Altarev *et al.*, Phys. Lett, **B276** (1992) 242.
- [22] K. Abdullah *et al.*, Phys. Rev. Lett. **65** (1990) 2347.

- [23] For reviews on the electron EDM in the standard model and in other models of CP violation, see, for example, S. Barr and W. Marciano in Ref. [13]; W. Bernreuther and M. Suzuki, Rev. Mod. Phys. **63** (1991) 313.
- [24] Private communication from E. Hinds.
- [25] A different method, making use of the relation between the nucleon matrix elements of the u and d quark EDM amplitude and the β -decay axial current matrix elements, was employed in Ref. [13] to obtain the neutron EDM from the perturbative expression of the quark EDM. This method was used to obtain the estimate of Eq. (29). It would give a neutron EDM about half of the size estimated in Eq. (38).
- [26] For reviews on the neutron EDM in the standard model and in other models of CP violation, see, for example, S. Barr and W. Marciano in Ref. [13]; X.-G. He, B. McKellar and S. Pakvasa, Int. J. Mod. Phys. **A4** (1989) 5011, (E) *ibid* **A6** (1991) 1063.
- [27] For experimental reviews on this subject, see, N. Ramsey, Annu. Rev. Nucl. Part. Sci. **40** (1990) 1; J. Pendlebury, Annu. Rev. Nucl. Part. Sci. **43** (1993) 687.
- [28] B. Holdom, Phys. Rev. **D23** (1981) 1637.

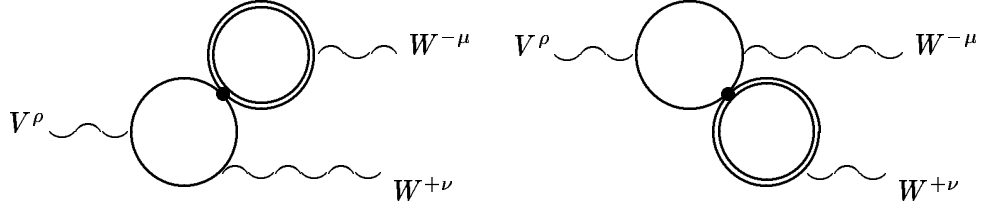


Fig. 1: CP-violating TGV's induced by the four-fermion operator \mathcal{L}_{4f}^2 in ETC theories. The single-line circle denotes a quark loop, the double-line circle denotes a techniquark loop. Diagrams with quark and techniquark loops interchanged are suppressed by a factor of $\mathcal{O}(\frac{m_i^2}{m_{TF}^2})$.

$$W_{\nu}^{-} \text{---} k \text{---} \bullet \text{---} k+p \text{---} W_{\mu}^{-} \quad \gamma_{\lambda} \text{---} p \text{---} \equiv -ie \Gamma_{\lambda\mu\nu}(k, p)$$

Fig. 2: The P- and CP-odd effective $WW\gamma$ vertex in momentum space. The W boson momenta here are arbitrary.

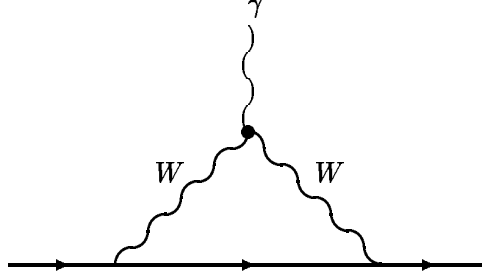


Fig. 3: The EDM of a fermion can be induced from the P- and CP-odd $WW\gamma$ effective vertex (denoted by the dark dot) generated by diagrams shown in Fig. 1. The induced fermion EDM is a two-loop effect in weak-coupling expansion.

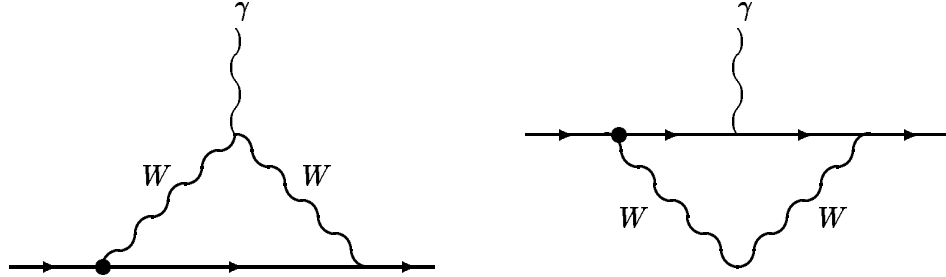


Fig. 4: The EDMs of the neutron and the electron can also be induced from the CP-violating $W\bar{f}_1 f_2$ vertex of Eq. (23) (extended to include the three quark-lepton families) at the one-loop level in weak coupling expansion, where f_1 and f_2 are the quarks or leptons of the first family. Because the ETC scale for the first family is two orders of magnitudes higher than for the third, the EDMs of the neutron and the electron generated from these one-loop diagrams are smaller than those induced from the P- and CP-odd $WW\gamma$ vertex shown in Fig. 3 — two-loop effects in the weak-coupling expansion. The effective, CP-violating $W\bar{f}_1 f_2$ vertex is denoted by the dark dot and can appear on either side of the fermion line.